Design and Demonstration of an Electronically Scanned Reflectarray Antenna at 100 GHz Using Multi-Resonant Cells Based on Liquid Crystals

Gerardo Perez-Palomino, Mariano Barba, José. A. Encinar, Robert Cahill, Raymond Dickie, Paul Baine and Michael Bain

***Abstract*—The design, fabrication and measured results are presented for a reconfigurable reflectarray antenna based on liquid crystals (LC) which operates above 100 GHz. The antenna has been designed to provide beam scanning capabilities over a wide angular range, a large bandwidth and reduced Side-Lobe Level. Measured radiation patterns are in good agreement with simulations, and show that the antenna generates an electronically steerable beam in one plane over an angular range of 55º in the frequency band from 96 to 104 GHz. The Side Lobes Level is lower than -13 dB for all the scan angles and -18 dB is obtained over 16% of the scan range. The measured performance is significantly better than previously published results for this class of electronically tunable antenna, and moreover verifies the accuracy of the proposed procedure for LC modeling and antenna design.**

***Index Terms*— Beam scanning reflectarrays, liquid crystal (LC), millimeter and sub-millimeter wave antennas, radar applications**

I. Introduction

LIQUID crystal-based reflectarrays are an attractive option for obtaining electronically reconfigurable antennas at frequencies above 60 GHz. With low fabrication costs and ease of integration [1], these antennas exploit the ability of liquid crystal material to change permittivity value by applying a quasi-static electric field, thus allowing the phase shift at each cell that composes the antenna to be configured.

In the literature, several unit cell geometries based on this tunable material have been designed and experimentally evaluated [2]-[8], which have led to the development of several different LC-based antenna arrangements [4]-[8]. In [4], 1-bit phase quantization was used to produce a switchable radiation pattern shape from sum to difference, whereas a continuous phase variation was used to implement a LC reflectarray with scanning capabilities in one plane at 35 GHz [5] and 77 GHz [6]-[7]. A LC-reconfigurable reflectarray at 78 GHz has been proposed in a folded configuration [8] to provide beam scanning in one plane with higher gain (25dBi). This arrangement uses a passive reflectarray to collimate the beam and to twist the electric field.

In these publications, the unit cells exhibit single-resonant behavior, therefore a small bandwidth is obtained. Furthermore, the bias voltage applied at each LC cell is obtained in [5]-[7] by using an algorithm based on measuring the received power and varying sequentially the voltages until maximum received power is obtained. In [4] and [8], the voltages are obtained by measuring the voltage dependence of the cells at one angle of incidence and for fixed cell dimensions. These procedures were employed because of the impossibility of measuring the phase curve versus voltage at each frequency, angle of incidence and for different cell dimensions, which is required to configure the appropriate phase-shift at each cell across the reflectarray surface. The algorithms that were used to design these antennas do not provide sufficient phase accuracy (besides being computationally intensive and inefficient), and therefore large phase errors that may be greater than 50º are produced across the aperture. These phase errors together with the amplitude ripple produced as consequence of the LC losses (which are voltage dependent), do not permit suppression of side-lobes to low levels and wide angle scanning. Therefore, the performance of these antennas in the best case is limited in terms of bandwidth (monochromatic), Side-Lobe Level (SLL) (-5 dB) and beam scanning range (20º), and therefore is not suitable for many practical applications with stringent requirements, such as radar or imaging.

In this communication, a reflectarray antenna that exhibits a better electrical performance than previously reported LC based structures is designed, fabricated and tested at frequencies centered at 100 GHz. The improvements are achieved by introducing two novel features. The first is the use of a multi-resonant architecture for the individual unit cells, which allows a broadband performance to be obtained. Although this type of cell has already been presented in [3], its behavior was only demonstrated at cell level and not when integrated into the antenna aperture in an array arrangement which is presented in this paper. The second novel feature employs a procedure to synthesize the required bias voltage at the unit cells, which does not require the use of measurement data and yet provides sufficient phase accuracy at each cell to obtain a good antenna performance in terms of side lobe level and scan range. Furthermore, this procedure also considers the effect of the amplitude ripple in the radiation pattern, which is minimized. Note that the design of a LC reflectarray antenna requires two separate procedures. The first one is the definition of the cell dimensions to maximise the phase range and bandwidth and to reduce the amplitude ripple as much as possible, which was carried out as described in [3]. However the most important challenge is to establish the voltages that should be applied at each unit cell with sufficient accuracy. The voltage synthesis proposed in this work enables the required voltages to be obtained by considering reflectarray elements with an arbitrary shape whilst it minimizes the effect of the amplitude ripple after the cells have been designed.

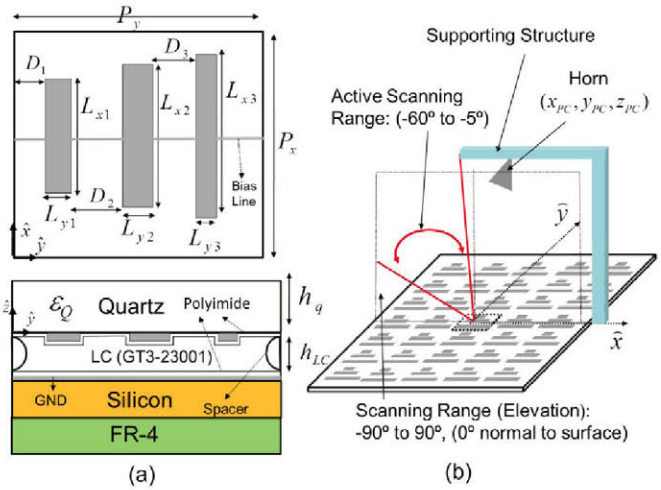

Fig. 1 Schematic of the LC-reflectarray. (a) Cells showing its different parts, (b) antenna configuration. Dimensions of the cells (mm): Py= 1.145, Px=1.093, Lx1=0.707. Lx2=0.748, Lx3=0.792, Ly1=0.20, Ly2=0.211, Ly3=0.20, D1=0.171, D2=0.096, D3=0.042, hq=550, hLC=0.075.

The proposed biasing strategy, the control circuitry and the signals to be used for biasing the LC are also described. The accuracy of the proposed design procedure is analyzed by comparing numerical simulations with measured radiation patterns, and by observing modifications to the beam shape which are attributed to variations of the amplitude and phase errors across the reflectarray aperture. This analysis at antenna level also permits an assessment of the viability of using multi-resonant cells to improve some features of the antenna performance other than the bandwidth, since amplitude ripple is a relatively important source of pattern distortion.

II. LC-BASED REFLECTARRAY DESIGN

A. Design of the LC-based reflectarray structure

The LC-based reflectarray antenna is composed of 54 x 52 multi-resonant cells each based on three parallel unequal length dipoles, which are printed on the lower surface of a 550 µm-thick quartz wafer. Fig. 1 shows a schematic of the reflectarray arrangement and the geometrical details of the cells. The ground plane is printed on the upper surface of a 1 mm thick metalized silicon wafer, and the 75 µm thick tunable layer is created by filling the cavity with LC which is inserted between the quartz and the silicon wafers. Several spacers are deposited across the entire surface of the reflectarray to maintain a uniform thickness LC cavity.

The dimensions of each cell have been adjusted to provide linear phase curves and sufficient phase range in the required frequency band at the corresponding angle of incidence, as described in [3]. The reflectarray phase center is located at the point (37.48, 0, 78.51) mm (see Fig. 1b), and a conical horn (Millitech SGH-08) is used as the primary feed. The horn has been modeled in CST Microwave Studio [9] in order to calculate the electromagnetic field across the aperture, which allows the actual incident field on the reflectarray surface to be

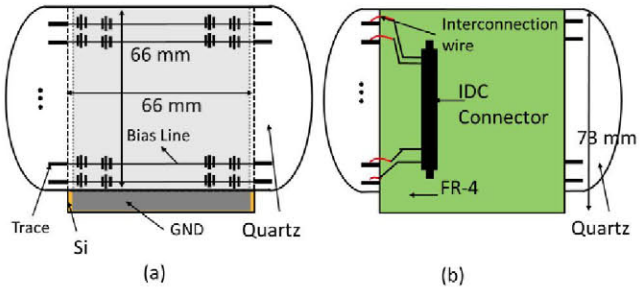

Fig. 2 Top (a) and bottom (b) views of the LC-based reflectarray showing details of its different parts.

obtained. The simulated horn gain is 21 dBi and the illumination level at the edges of the reflectarray is -12 dB. The dimensions of the cells are obtained by using the extreme states of the LC permittivity and the concept of isotropic effective permittivity to obtain good computational efficiency in the design [3]. For this antenna, the cells have been designed to exhibit low sensitivity to the angle of incidence, so that the dimensions, which are given in Fig. 1, can be made identical over the entire surface. The LC used is the mixture GT3-23001, which is manufactured by Merck and whose parameters are: $\varepsilon_{r//}$(100 GHz)=3.25, $\varepsilon_{r\perp}$(100 GHz)=2.47, $\tan\delta_{//}$(100 GHz)= 0.015, $\tan\delta_{\perp}$(100 GHz)= 0.02 (measured in [10]), and $\varepsilon_{r//}$(1 KHz)=8.1, $\Delta\varepsilon$ (1 KHz)=4.6 (given by Merck).

The cells exhibit experimental linear phase curves in the band from 96 to 104 GHz, with a maximum phase error of ±35° (at 104 GHz), and the phase-range from zero to maximum bias voltage is 330°, which is sufficient to collimate the beam. The magnitude of the reflection coefficient, mainly attributed to the absorption losses of the liquid crystals, has different values across the antenna surface (amplitude ripple). This ripple is around 2 dB in the band from 96 to 102 GHz and increases up to 9 dB at 104 GHz, which is lower than provided by single resonant cells. The simulated and measured reflection phase and losses of these cells are reported in [3] and [11].

B. Scanning Capabilities and Voltage Addressing

To simplify the control circuitry and the structure to bias the cells, the LC reflectarray is only biased by rows, so that the scanning can be performed in one plane (elevation). For this feed arrangement, the reflectarray is only able to focus the beam in one plane (the scanning plane), therefore the radiation pattern in the azimuth plane will be similar in shape to that provided by the horn. Since the beam is collimated and scanned in the elevation plane, the gain will be lower than that obtained from a pencil beam; however the voltage addressing is greatly simplified.

Each cell is composed of three printed dipoles and a 30 µm-wide biasing line that interconnects the dipoles, and works as an electrode to apply the ac bias signals. The biasing lines protrude beyond the active area into 0.5 mm-width rectangular traces which are used to connect the bias lines of each row to the control circuits (see Fig. 2a). An additional layer of FR-4 (3 mm thick) was glued to the lower surface of the silicon wafer, which supports the ac lines and the bias connectors (see Fig. 1a

and Fig. 2b).

Each of the bias lines is connected from the quartz to the corresponding trace printed on the FR-4 layer, by a wire (0.1 mm) that is soldered, and each one of the traces is connected to the pin of a IDC connector that serves as an interface between the LC device and the control circuits (see Fig. 2b).

C. *Biasing and Voltage Synthesis for the cells*

After the geometrical dimensions of the identical unit cells are obtained, calculation of the voltage dependence (reflection phase and amplitude curves versus voltage) is obtained with high accuracy in order to achieve good performance in terms of side-lobe level and scanning range. Here, the required accuracy is achieved by modeling the LC as an anisotropic stratified media in one dimension [11], which allows the voltage dependence of each cell to be obtained from simulations. This numerical model takes into accounts the LC elastic parameters, the LC dielectric anisotropy at both the RF and ac biasing frequencies, and the waveform of the bias signals.

The biasing has been selected to be sequential in order to reduce the complexity of the control circuits. This strategy requires the use of a retention RC circuit at each bias line (see Fig. 3), which must be designed to maintain the corresponding fixed voltage until the next refresh of the line.

Note that RC circuits require the use of DC or square signals for biasing. Here, a square signal with zero offset is selected in order to reduce as much as possible the dynamic effects that perturb the permittivity when the LC is excited by a quasi-DC signal [12]. The refreshing period in this case would be T=2*Tp*Nv, where Nv is the total number of voltages used and Tp is the actuation time of a voltage, which must be greater than the delay of the switching circuits plus the required time to fully charge the capacitor until the desired value is obtained. Note that lines with the same voltage are biased at the same time.

In our case, the number of voltages selected is 20, whereas the time delay of the switches (relays) is 10 milliseconds. Thus, assuming a safety margin time of 64 ms to ensure the correct charge of the RC circuits, the design would lead to a square signal of 0.33 Hz-frequency (T=2*74 ms*20=2.96 s). The switches that select the lines are controlled by TTL signals that are produced by a computer, whereas the sequence of pulses S(t) is generated by the control circuits (see Fig. 3). Note that the selected refreshing period can limit the scanning speed of the antenna, although both the switching time of the relays and the safety margin times, can be drastically reduced. In our case, these times have been selected to reduce the cost and the complexity of the demonstrator. However, the scanning speed is usually limited by the LC dynamics, since the decay time depends on the viscosity and the LC layer thickness, which is relatively thick in microwaves. In this case, the scanning speed has been estimated to be 2 s, which makes this antenna usable for many applications including Earth observation instruments and climate monitoring radiometers. To reduce the switching times for a fixed LC thickness, several strategies can be employed, including the use of dual frequency LCs, polymer network LC (PNLC) or more complex biasing arrangements [12]. All these strategies have reported time reductions of

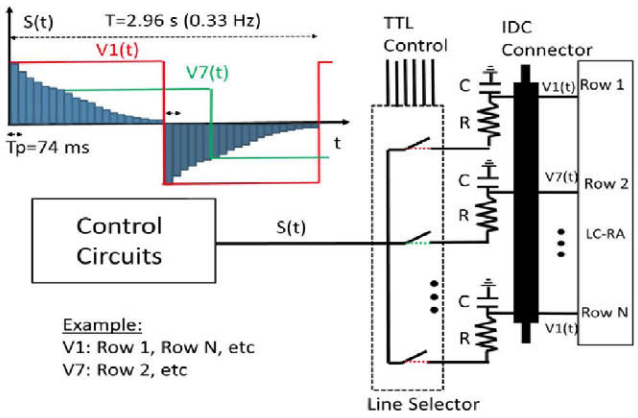

Fig. 3 Schematic of the retention circuits that maintain a fixed voltage applied to the LC together with the applied signals.

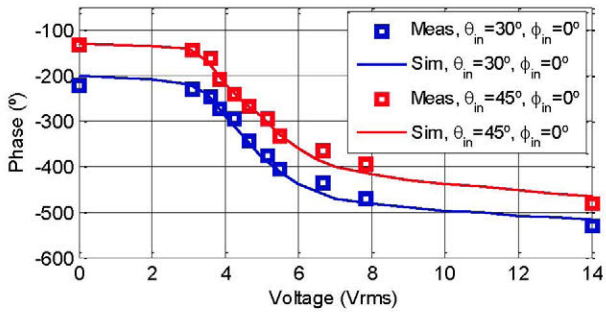

Fig. 4 Phase of the reflection coefficient (100 GHz) of the cells as a function of the rms voltage at two angles of incidence for the case where the bias signal applied to the LC is 0.33 Hz-square.

several orders of magnitude when used in LC displays.

Once the biasing strategy has been selected, the LC modeling requires a knowledge of the dielectric anisotropy, $\Delta\varepsilon_r=\varepsilon_r//-\varepsilon_r\perp$, at the frequency of the bias signal (0.33 Hz). However, generally this is only provided by manufacturers at 1 KHz. Therefore, this parameter must be measured. The fabricated prototype has been used to extract the dielectric anisotropy $\Delta\varepsilon_r$, at the bias frequency from RF measurements, by solving the inverse problem to that presented in [11] to model the LC. The method is based on measuring the reflection coefficient of the reflectarrays cell (at 100 GHz) at a fixed angle of incidence (periodic environment) and at a defined voltage for the case that the LC is biased with the 0.33 Hz signal; once the data acquisition is completed, and since the dielectric anisotropy is the unknown, the reflection phase of the cell is calculated iteratively, so that the value of $\Delta\varepsilon_r$ is varied for each iteration until the simulated phase reaches the values measured. In our case, a numerical analysis code based on the Spectral-Domain Method of Moments (SD-MoM) for anisotropic stratified media has been used to simulate the structure.

As a general observation, although theoretically the measurement of a single voltage is enough to obtain $\Delta\varepsilon_r$, the existence of errors (due to manufacturing tolerances, convergence of the numerical e.m. simulations, etc) means that a single voltage measurement does not provide a particular accurate value for the dielectric anisotropy. Thus, the measurements should be carried out for different voltages. In

our case, five different phase acquisitions were done at a fixed angle of incidence (θ=45°, φ=0°), so five values of the dielectric anisotropy were obtained, and the average $\Delta\varepsilon_r$(0.33 Hz)=5.72 is used. The accuracy of the extracted value of $\Delta\varepsilon_r$(0.33 Hz) is estimated to be ±0.15 for the multi-resonant structure with the maximum dimensional tolerances associated with the fabrication process assumed, but this can be increased up to ±0.4 when the errors are systematic. The dielectric anisotropy at RF also has an influence on the accuracy of the method used. However, an FSS has previously been used to extract this parameter above 100 GHz [10], and since the LC does not present transversal inhomogeneity, the values obtained for $\Delta\varepsilon_r$(100 GHz) are considered to be sufficiently accurate. The uncertainty associated with the value of $\Delta\varepsilon_r$(0.33 Hz) can produce average phase errors after voltage synthesis, of around ±10°.

Once the value of $\Delta\varepsilon_r$(0.33 Hz) is obtained, it can be used to calculate the voltage dependence of all the unit cells of the reflectarray, in order to obtain the voltage distribution which should be applied to obtain the required radiation pattern (voltage synthesis). To evaluate the accuracy of the extracted value, $\Delta\varepsilon_r$(0.33 Hz), the voltage dependence for two different angles of incidence, θ=45°, φ=0° and θ=30°, φ=0°, has been calculated and measured in a quasi-optical bench. The results at 100 GHz are plotted in Fig. 4, which shows that the phase versus voltage plot is closely predicted. Note that the average phase error is close to value expected (around 10°) at 100 GHz and the maximum error is 23°.

Since the beam is scanned in one plane, the voltage synthesis is obtained for the cell located at the center of each row. This voltage is calculated for the corresponding cell by simulating the reflection phase at a certain test voltage, and then by comparing both the calculated and the required phases. This process is repeated iteratively until a tolerable phase error threshold is reached. Each iteration of each cell is simulated by using a code based on MoM for anisotropic stratified media, whereas the required phase-shift is obtained analytically [13] and is calculated at each angle at the design frequency (100 GHz).

Note that if ideal phase shifters are considered, the required phase for a specified scan angle can be increased by adding an arbitrary phase constant, C, without any distortion of the radiation pattern. However, the existence of amplitude ripple in the reflection coefficient of the cells implies that each value of C provides a different radiation pattern, so that there is an optimum value for this parameter which gives the best radiation patterns for a defined electrical criterion (gain, side lobes level, or both together). This fact is not significant if the amplitude ripple on the reflectarray is low (i.e. passive reflectarrays); however, the ripple in our case is relatively high so this effect must be taken into account in the voltage synthesis. Thus, the voltage synthesis of the entire reflectarray for a given scan angle is introduced in an optimization process. In this process, C is the variable to be optimized, the objective is to minimize the side lobes level and the iterations involve calculation of the resulting radiation pattern. Note that this process is able to reduce as much as possible the effect of the amplitude ripple after the cells have been designed. The dependence of the SLL on C entails a large number of local minima, so an appropriate initial point (C0) must be chosen to make the convergence efficient. Here, the value of C0 has been obtained by previously calculating several points on the SLL curve using the homogeneous effective tensors defined in [11].

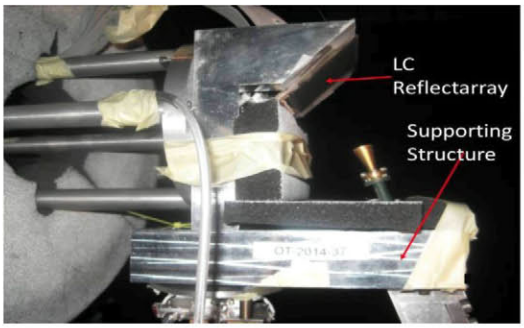

Fig. 5 Photograph of the single offset LC based reflectarray antenna

III. Measurements and Discussion

The radiation patterns of the LC-based reflectarray antenna have been measured in an anechoic chamber for several scan angles and frequencies about the nominal design frequency of 100 GHz. Fig. 5 shows a photograph of the antenna placed in the anechoic chamber. The reflectarray has been placed on an aluminum support structure, which was covered with absorber material in order to avoid undesired reflections. The location of the feed-horn and the support structure provide a region potentially free of blockage within the range from -90° to -5° (see Fig. 1). The angles beyond -60° require sharp phase variations (in addition to high scan loss), and the phase errors as consequence of using the local periodicity approach, produce a significant increase in the side lobe level. Therefore, the scanning range considered here is from -60° to -5° (see Fig. 1), although it could be improved using a more appropriate support structure or even other location of the horn.

Fig. 6- 8 show the experimental results in the elevation plane for six scan angles (-60°, -45°, -35°, -25°, -15°, -5°) at 100 GHz and the lower and upper frequencies selected for this measurement campaign, 96 and 104 GHz. As can be seen in Fig. 6, the reflectarray antenna provides a steerable beam in one plane over a wide angular range (55°) at 100 GHz. The side lobe level is lower than -13 dB for all the scan angles, and the pointing errors are negligible. The side lobe level are lower than -18 dB from -15° to -25°, but increase when the beam is scanned away from the specular direction (-25°). The fact that the side lobes level is low over a relatively large angular range is mainly due to the small phase errors on the reflectarray surface. As previously mentioned, the average phase error at the design frequency is around 10°. In this case, the main source of pattern distortion is the amplitude ripple, which is reduced at 100 GHz using the aforementioned numerical design technique. The accuracy of the proposed design procedure is also evident in the prediction of the radiation patterns. This can be seen in Fig. 9, which shows the measured radiation pattern in the elevation plane for the beam scanned at -25° (solid line) compared with

simulations at the design frequency, 100 GHz. The radiation pattern obtained from ideal phase shifters is represented by the dotted curve in Fig. 9 as a reference, and the dashed curve represents the simulated radiation pattern by considering the actual reflections from the surface of the LC-based reflectarray. As can be seen, there is good agreement between measurements and simulations. The discrepancies are similar to these obtained for passive reflectarrays.

At 96 and 104 GHz the phase errors inherently increase, since the phase behavior of the cells is not perfectly linear with frequency and the voltage synthesis is obtained at 100 GHz. At 96 GHz the phase error and the amplitude ripple are low, so the electrical performance of the antenna at this frequency is similar to that obtained at 100 GHz (see Fig. 7). This behavior is maintained in the band from 96 to 102 GHz. However, the phase errors and the ripple at 104 GHz increase up to 60° and 9 dB, respectively, and this produces an increase in the side lobes levels which peak at -6.5 dB (see Fig. 8). Note that the increase in the side lobes is especially high for the lobe that corresponds to the specular direction [14].

To evaluate the impact on the antenna performance of the amplitude ripple and the phase errors, further analysis is presented at 104 GHz. The measured (solid line) radiation pattern for the beam scanned to -5° is compared in Fig.10 with the simulations obtained using different assumptions. The dotted curve represents the pattern assuming ideal phase shifters. The dash-dot curve plots the simulations using the actual reflection amplitude from the surface of each of the LC cells, but assuming ideal phase curves (zero phase error), whereas the simulations that consider the real effect of the LC-based cells (amplitude and phase) are represented by the dashed curve. It is observed that the amplitude ripple produces an increase in the side-lobe level although to a lesser extent than the phase errors, which are primarily responsible for the distortions observed in the radiation patterns. Concerning the bandwidth, if the criterion of 3 dB gain reduction from the peak value is assumed, the antenna is shown to meet this specification from 96 to 102 GHz. In this range, the SLL is below -13 dB for all the scan angles. Table I shows that the electrical performance for the antenna design presented in this paper is significantly better than previously published results for LC-based reflectarrays.

It should be noted that the voltage synthesis is reconfigurable also in frequency, so it can be calculated independently at each frequency. Thus, the phase errors produced in the band from 102 to 104 GHz as a consequence of the non-linearity of the phase curves could be compensated by obtaining suitable bias voltages which could be used to improve the antenna performance at each frequency, although this method would reduce the instantaneous bandwidth of the antenna. Note also that the design procedure to calculate the voltages could be modified to find an optimized full band voltage distribution that considers the edge and the center design frequencies.

Concerning the antenna gain reduction (the efficiency is 18.5 %) observed in Fig. 9 and 10, note that it can be attributed to the high LC absorption losses, the amplitude ripple and the phase errors. To evaluate the contribution of each of these factors,

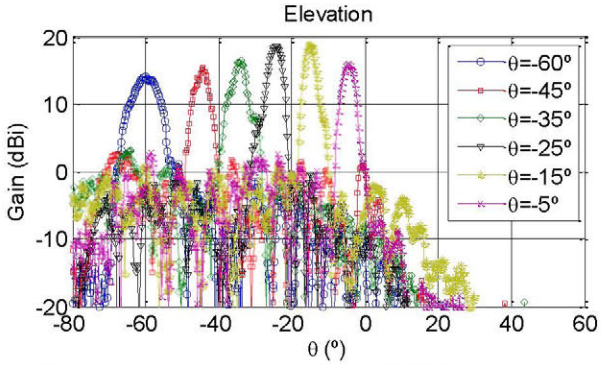

Fig. 6 Measured elevation radiation patterns at 100 GHz of several scan angles

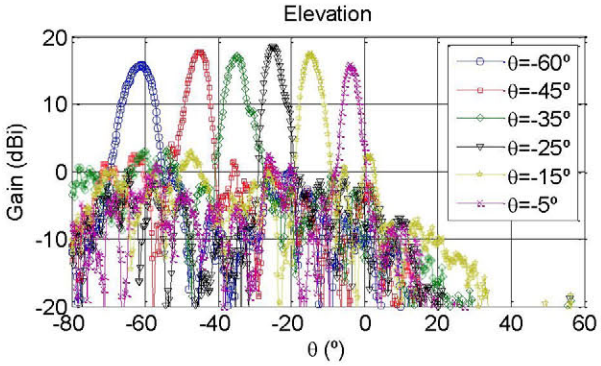

Fig. 7 Measured elevation radiation patterns at 96 GHz of several scan angles

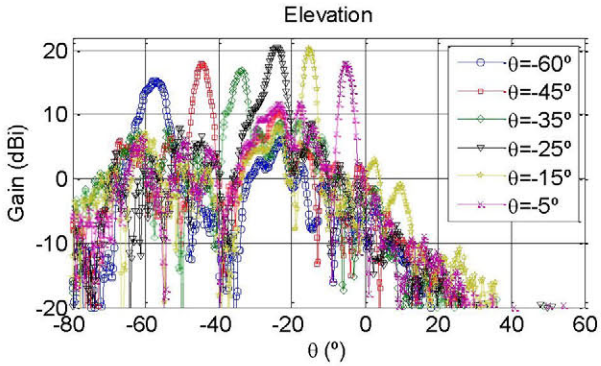

Fig. 8 Measured elevation radiation patterns at 104 GHz of several scan angles

TABLE I
COMPARISON OF ELECTRICAL PERFORMANCE OF LC-REFLECTARRAYS

Feature	Ref [5]	Ref [6]	Ref [7]	Ref [8]	This Work
Frequency (GHz)	35	77	77	78	96-102
Max Gain (dBi)	19.5	-	-	25.1	19.4
Scanning Capabilities	1-D	1-D	1-D	1-D	1-D
Scanning Range (°)	35	35	20	12	55
SLL (dB)[1]	-4	-3	-5	-6	-13
Polarisation	Linear	Linear	Linear	Linear	Linear
Antenna Structure	Single	Single	Single	Folded	Single

[1] In the entire scanning range and bandwidth

Fig. 11 shows the measured and simulated gain at 100 GHz for different scan angles. The simulations consider three cases: ideal phase-shifters, cells without losses and the actual phase (Ph), and cells providing the actual reflection coefficient in

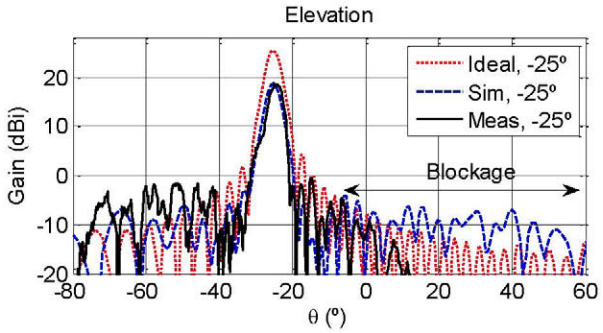

Fig. 9 Measured (Meas) and simulated (Sim) elevation radiation patterns at 100 GHz for the beam scanned to -25° in elevation. The ideal radiation pattern is also plotted. Simulation considers the actual reflection coefficient of the cells.

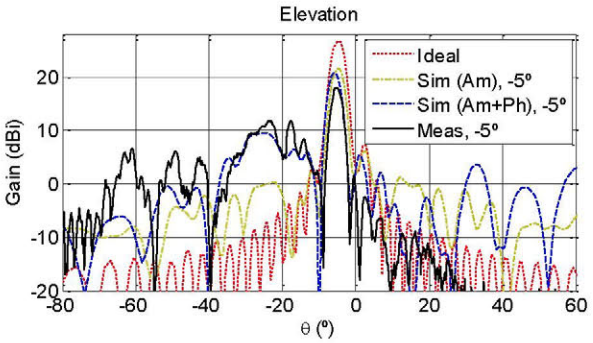

Fig. 10 Measured (Meas) and simulated (Sim) elevation radiation patterns at 104 GHz for the beam scanned to -5° in elevation. The ideal radiation pattern is also plotted. Simulations consider the actual reflection coefficients of the cells (Am+Ph) or cells providing ideal phases and actual amplitudes (Am)

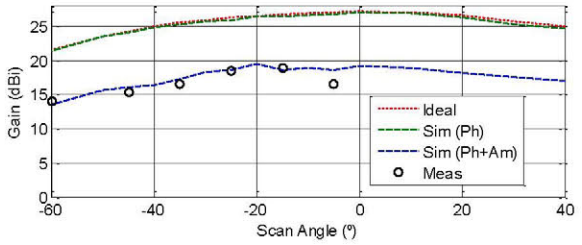

Fig. 11 Measured (Meas) and simulated (Sim) gain at 100 GHz with respect to the scan angle – simulations assume the reflection coefficient of the cells under certain considerations given in the text.

amplitude and phase (Am+Ph). The plots show that the main contribution to the gain reduction is the absorption loss of the LC, whereas the phase errors represent a small contribution which peaks around 1 dB at 104 GHz (Fig. 10). The results also show that the ideal gain curve (Fig. 11) exhibits a maximum beam scan loss of 6.5 dB at -60°. The loss attributed to the phase errors and reflection magnitude is fairly constant with angle at 100 GHz, although the actual gain curve also shows the amplitude ripple, which makes that at a certain scan angle, the gain at 96 and 104 GHz is different than that obtained at 100 GHz. It should be mentioned that to obtain a higher gain using the same LC material, the antenna aperture could be increased (which is easily implementable for this type of antenna), or other architectures can be considered: dual reflector antenna [15], or a single offset antenna but with 2D voltage addressing. In any case, the losses of the LC can also be reduced, which is being achieved with the development of new LC mixtures [16].

IV. Conclusions

A single-offset reconfigurable reflectarray antenna based on electronically reconfigurable liquid crystals has been designed, fabricated and measured at three frequencies centered at 100 GHz. The experimental radiation patterns are in good agreement with simulations, and show that the antenna generates an electronically steerable beam in one plane over an angular range of 55° and the gain reduction is less than 3 dB within the frequency band 96 to 102 GHz. The side lobe levels are lower than -13 dB for all the scan angles. The electrical performance validates the accuracy and viability of the LC modeling, the unit-cell used and the voltage synthesis proposed.

Acknowledgment

The authors are grateful to Merck KGaA in Darmstadt for supplying the GT3-23001 liquid crystal material.

References

[1] S. V. Hum and J. Perruisseau-Carrier, "Reconfigurable Reflectarrays and Array Lenses for Dynamic Antenna Beam Control: A Review," *IEEE Trans. Antennas Propagat.*, vol. 62, no. 1, pp. 183-198, Jan. 2014.

[2] W. Hu, et al, "Design and Measurement of Reconfigurable Millimeter Wave Reflectarray Cells With Nematic Liquid Crystal," *IEEE Trans. Antennas Propagat.*, vol. 56, no. 10, pp. 3112-3117, Oct. 2008.

[3] G. Perez-Palomino, et al., "Design and Experimental Validation of Liquid Crystal-Based Reconfigurable Reflectarray Elements With Improved Bandwidth in F-Band," *IEEE Trans. Antennas Propagat.*, vol. 61, no. 4, pp. 1704-1713, Apr. 2013.

[4] W. Hu, et al, "Liquid-crystal-based reflectarray antenna with electronically switchable monopulse patterns," *Electron, Lett.,*, vol. 43, no. 14, pp. 744-745, 2007.

[5] A. Moessinger, et al., "Electronically reconfigurable reflectarray with nematic liquid crystal," *Electron. Lett.*, vol. 42, no. 16, pp. 899-900, Aug, 2006.

[6] R. Marin, et al, "77 GHz reconfigurable reflectarray with nematic liquid crystal," in Proc. 2nd EuCAP, Edinburgh, Nov. 2007.

[7] S. Bildik, et al., "Reconfigurable Liquid Crystal Reflectarray with Extended Tunable Phase Range" in Proc. 8th EuRAD, Manchester, Oct. 2011.

[8] S. Bildik, et al.,"Reconfigurable Folded Reflectarray Antenna Based Upon Liquid Crystal Technology," *IEEE Trans. Antennas Propagat.*, vol. 63, no. 1, pp. 122-132, Jan. 2015

[9] CST Microwave Studio. [Online]. Available: http://www.cst.com.

[10] R. Dickie, et al., "Electrical characterisation of liquid crystals at millimetre wavelengths using frequency selective surfaces" *Electron Lett.*, vol. 48, no. 11, pp. 611-612, May. 2012.

[11] G. Perez-Palomino, et al., "Accurate and Efficient Modeling to Calculate the Voltage Dependence of Liquid Crystal Based Reflectarray Cells," *IEEE Trans. Antennas Propagat.*, vol. 62, no. 5, pp. 2659-2668, May. 2014.

[12] Deng-Ke Yang and S. T. Wu, *Fundamentals of Liquid Crystal Devices.* 2nd ed. Willey, 2015.

[13] J. Huang and J. A. Encinar, *Reflectarray Antennas.* Wiley, 2007.

[14] R. El Hani, and J. J. Laurin, "Specular Reflection Analysis for Off-Specular Reflectarray Antennas," *IEEE Trans. Antennas Propagat.*, vol. 61, no. 7, pp. 3575-3581, Jul. 2013.

[15] W. Hu, et al, "94 GHz Dual-Reflector Antenna With Reflectarray Subreflector," *IEEE Trans. Antennas Propagat.*, vol. 57, no. 10, pp. 3043-3050, Oct. 2009.

[16] A. Manabe, "Liquid Crystals for microwave applications,", in Proc 7th European Conference on Antennas and Propagation, EUCAP, p.p. 1973-1974. Gothenburg, 2013,